Seismic Image Mispositioning in the Depth-Angle Domain

Ernesto Bonomi
EIS-CRS4

From the 2D phase-shift extrapolation of two oriented waves, down-going and up-going, using the relation between k_h, the horizontal offset wavenumber, and k_z, the vertical one, I compute the true position of the image point lying on a reflecting surface with dip angle α. The resulting coordinates take into account the orientation of the slowness vectors $\mathbf{p_s}$ and $\mathbf{p_r}$ with scattering angle 2θ, one describing the down-going wave and the other the up-going one.

In this framework, I can show that a wrong estimate of the migration velocity causes the displacement and, then, the mispositioning of the image point along the normal to the reflector. I derive the well-known expression of the vertical residual moveout in the (z, θ)-domain with respect the true coordinate.

Similarly, the image point displacement happens when the time of flight t_0 is not correctly identified as a primary echo. Assuming a planar reflector and substituting t_0 with t_m, the time of flight of a multiple event of order m, I derive in the (z, θ)-domain the general residual moveout expression.

Part I: Oriented migration of the impulsive response

Wave propagation in the phase-space $(\mathbf{x}, \mathbf{p})$

Phase-space wavefield: V, the pressure field, is not only a function of position $\mathbf{x} = (y, z)^\top$ and time t, but also of $\mathbf{p} = (p_y, p_z)^\top$, the wavefront *orientation* which must satisfy $||\mathbf{p}|| = n(\mathbf{x})$, the *eikonal equation*; n denotes the slowness function.

Oriented waves in homogeneous media: Fomel's formulation (2003) of the one-way depth propagation in 2D takes the form

$$\frac{\partial \hat{V}_{p_y}}{\partial z} = \imath k_z \, \hat{V}_{p_y} \;, \quad k_z = \frac{\omega n^2 - k_y p_y}{p_z} \;, \quad p_z = \sqrt{n^2 - p_y^2} \;, \tag{1}$$

leading to the usual *phase-shift* formula

$$\hat{V}_{p_y}\left(k_y, z + \triangle z, \omega\right) = e^{\imath k_z \triangle z} \, \hat{V}_{p_y}\left(k_y, z, \omega\right) \;, \tag{2}$$

that I shall use to independently *extrapolate* the impulsive signal of a pair source-receiver to image a scattering point lying on a reflecting surface.

Depth extrapolation

Both source and receiver wavefronts collide with a scattering angle 2θ on a reflecting point lying on a surface with dip angle α:

$$\mathbf{p_s} = n\left[\sin(\alpha+\theta), \cos(\alpha+\theta)\right]^\top, \quad \mathbf{p_r} = n\left[\sin(\alpha-\theta), \cos(\alpha-\theta)\right]^\top . \tag{3}$$

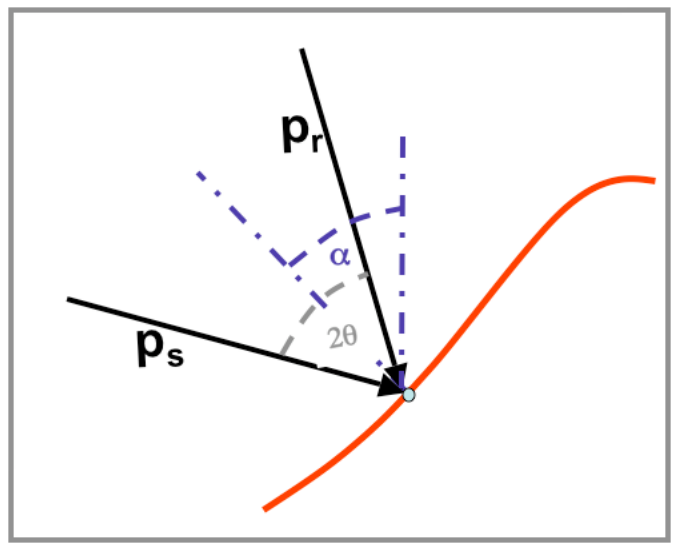

Figure 1: Source and receiver depth extrapolation: wave scattering

Homogeneous media

Using twice Eq.(1), the extrapolation of both source and receiver - with the help of (2) and (3) - leads to the vertical wave number expression or *dispersion relation:*

$$k_z = \frac{2\omega n \cos\alpha \cos\theta}{\cos^2\alpha - \sin^2\theta} - \frac{k_m \sin\alpha\cos\alpha - k_h \sin\theta\cos\theta}{\cos^2\alpha - \sin^2\theta} \ ; \tag{4}$$

$k_h = k_r^{(1)} - k_s^{(1)}$ and $k_m = k_r^{(1)} + k_s^{(1)}$ are the offset and the midpoint wave numbers.

Remark: In a homogeneous medium, we have $\mathbf{p_s} = \mathbf{k_s}/\omega$ and $\mathbf{p_r} = \mathbf{k_r}/\omega$, so that:

$$\omega\left(\mathbf{p_s} + \mathbf{p_r}\right) = \left(k_m, k_z\right)^\top \ ,$$

where, with the help of (3),

$$k_m = 2n\omega \sin\alpha\cos\theta \ , \qquad k_z = 2n\omega\cos\alpha\cos\theta. \tag{5}$$

After substitution of (5) into (4), we derive the fundamental relation, already suggested by Stolt and Weglein (1985), relating, *independently* of the reflector deep, offset and vertical wave numbers through the tangent of the scattering angle:

$$\frac{k_h}{k_z} = -\tan\theta \ . \tag{6}$$

Ray trajectory: three useful relations

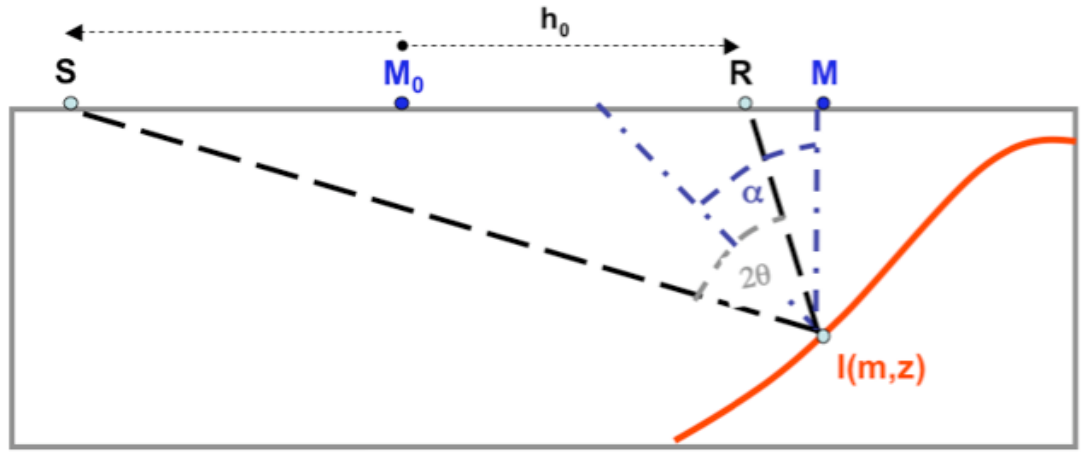

Figure 2: Ray trajectory and geometric parameters

Providing the coordinates (m_I, z_I) of the scattering point I and the dip angle $\alpha = \alpha_I$, the time of flight and the acquisition setup may be derived in terms of θ:

$$\frac{t_0}{2n} = \frac{\cos\alpha_I \cos\theta}{\cos^2\alpha_I - \sin^2\theta}\, z_I, \quad h_0 = \frac{\sin\theta\cos\theta}{\cos^2\alpha_I - \sin^2\theta}\, z_I, \quad m_I - m_0 = \frac{\sin\alpha_I \cos\alpha_I}{\cos^2\alpha_I - \sin^2\theta}\, z_I, \tag{7}$$

where m_0 is the midpoint, h_0 the offset and t_0 the time of flight of the signal.

Remark: to avoid the discontinuity and to keep $t_o > 0$, we need $|\theta| < \pi/2 - |\alpha_I|$.

Image in the midpoint-angle domain of the medium impulsive time response

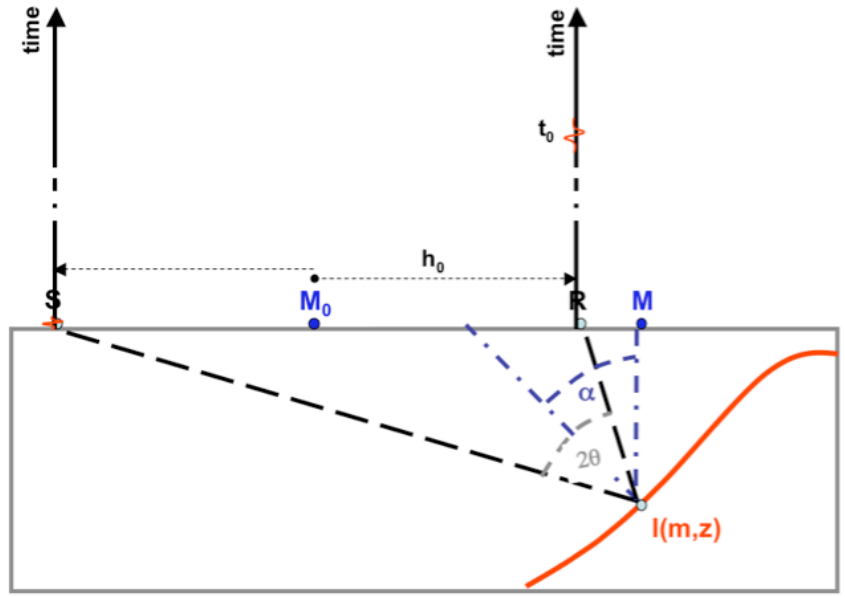

Figure 3: Acquisition of a single trace

The initial condition for the depth extrapolation algorithm defined by (2) takes the form

$$\hat{\mathcal{T}}(k_m, k_h, 0, \omega) = e^{\imath[(m-m_0)k_m+(h-h_0)k_h-\omega t_0]} \ . \tag{8}$$

Remark: k_z in the midpoint-offset domain is given by Eq.(4).

Depth imaging: after having applied the phase-shift formula (2) to the initial condition (8), we find a subsurface image for each offset h:

$$\mathcal{I}(m,h,z) = \int d\omega \; dk_m \; dk_h \; \hat{\mathcal{I}}(k_m,k_h,0,\omega) \; e^{\imath k_z z} \;, \quad k_z = k_z\,(k_m,k_h,\omega) \;. \tag{9}$$

To eliminate h, using relation (6) between offset and vertical wave numbers, the resulting image (9) must be Fourier transformed:

$$\hat{\mathcal{I}}(m,\kappa_h,\kappa_z) = \int dz \; dh \; \mathcal{I}(m,h,z) \; e^{-\imath(\kappa_h h + \kappa_z z)} \;, \quad \kappa_h = -\,\kappa_z \tan\theta \;. \tag{10}$$

Midpoint-angle domain: after the inverse transform of (10) along κ_z, we find the desired image volume corresponding to the impulsive response of the time section:

$$\begin{aligned} I_\alpha(m,z,\theta) \;\; = \;\; & \frac{\left|\cos^2\alpha - \sin^2\theta\right|}{2n\cos\alpha\cos\theta} \; \delta\left[(m-m_0) - \frac{t_0}{2n}\frac{\sin\alpha}{\cos\theta}\right] \times \\ & \delta\left[(z + h_0\tan\theta) - \frac{t_0}{2n}\frac{\cos\alpha}{\cos\theta}\right] \;. \end{aligned} \tag{11}$$

Geometric locus of the migrated event

Geometric locus: the support of Eq.(11) is a circle of center $(m_0, -h_0 \tan\theta)$ and radius $t_0/(2n\cos\theta)$ collecting all potential image points (m, z):

$$m = m_0 + \frac{t_0}{2n}\frac{\sin\alpha}{\cos\theta} \ , \quad z = -h_0\tan\theta + \frac{t_0}{2n}\frac{\cos\alpha}{\cos\theta} \ . \tag{12}$$

Remark: θ is the actual variable controlling the acquisition midpoint, the offset and the time of flight, Fig.(3).

True image point: providing the correct deep, $\alpha = \alpha_I$, after the substitution into (12) of the proper values of m_0, h_0 and t_0 provided by (7), we find the expected result *independent* of θ:

$$m = m_I \ , \quad z = z_I \ . \tag{13}$$

These two relations define the *tangent* point of all circles, one for each value of θ, as illustrated in Fig.(4).

(True) amplitude: Eq.(11) shows that the amplitude of the image point remains a function of the scattering angle θ, with $|\theta| < \pi/2 - |\alpha_I|$, Fig(5).

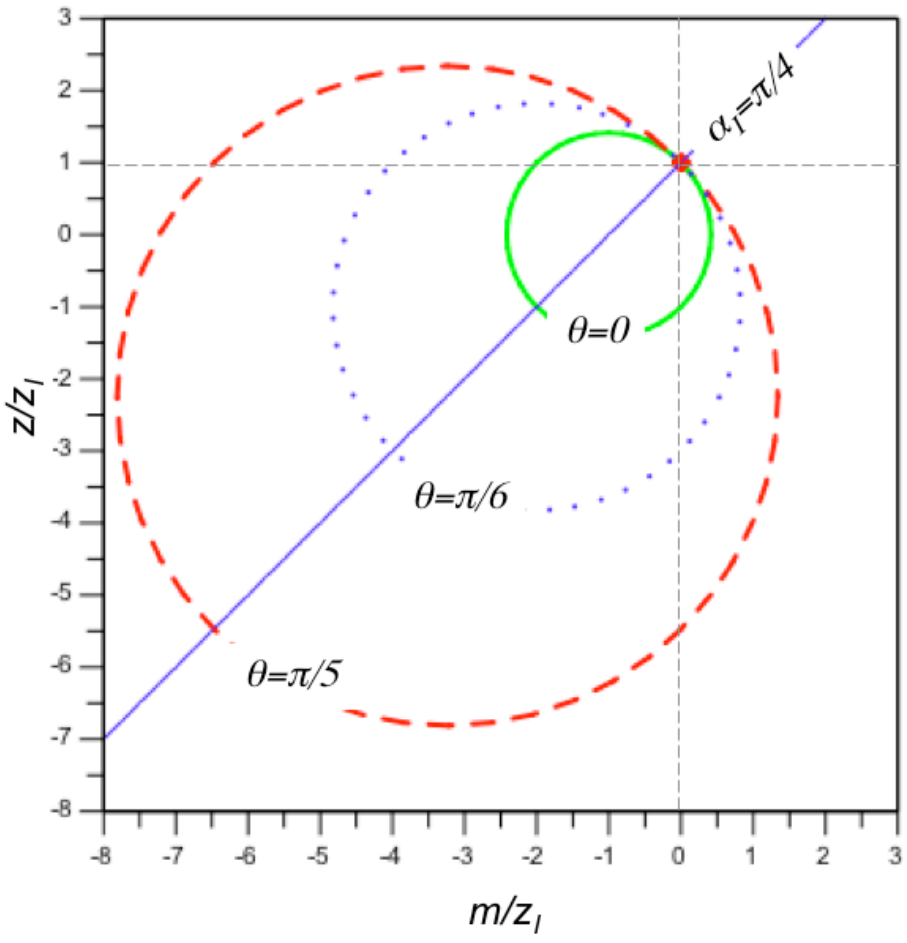

Figure 4: Geometrical locus of all potential image points, plotted here for three values of θ: when the dip angle α tends to α_I, all circles becomes tangent in I

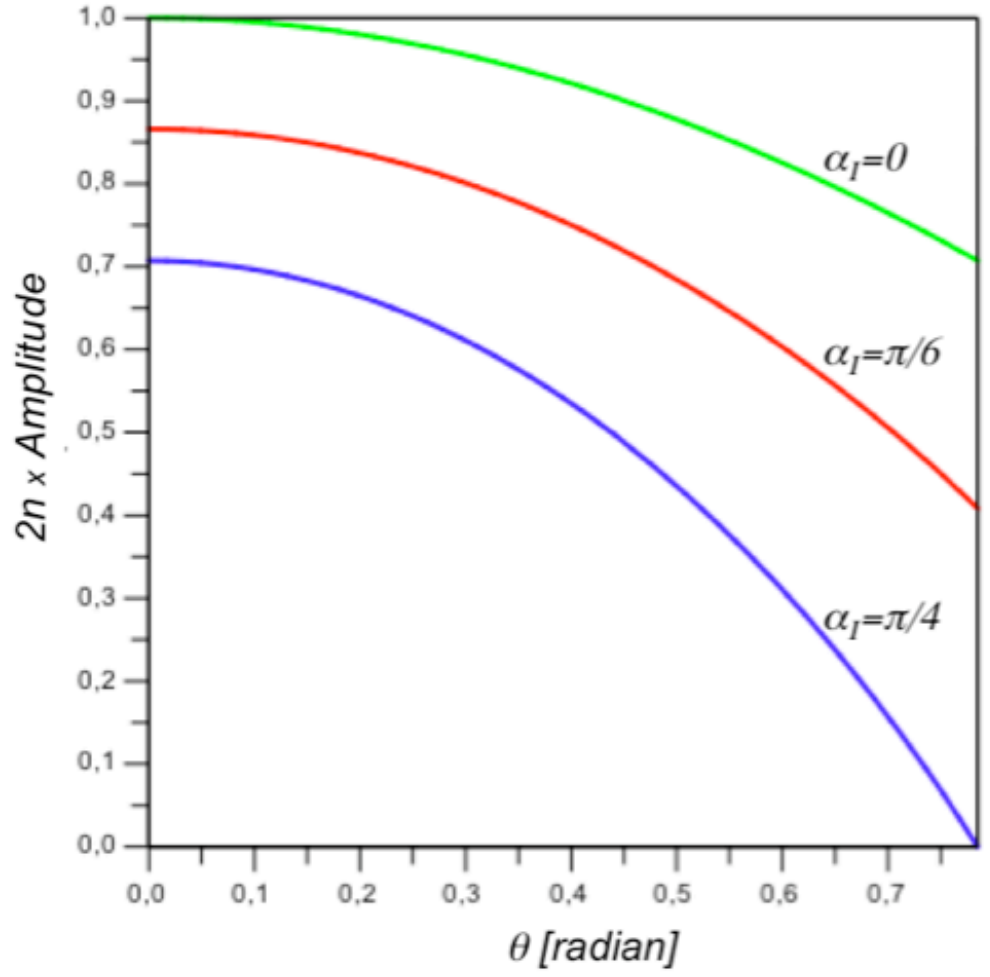

Figure 5: Amplitude of the image point: a decreasing function of the scattering angle

Part II: Improper migration slowness and image mispositioning

Migration with a wrong migration slowness: image mispositioning

So far, we have assumed the value of n is exact. This guarantees the exact correspondence between the reflecting point and its migrated image, Eq.(13).

Wrong migration slowness: Eqs.(12) show that the *incorrect* estimate of the slowness n_ρ modifies the *radius* of the each circle in the image volume, leaving untouched its center:

$$(m - m_0)^2 + (z + h_0 \tan\theta)^2 = \left(\frac{t_0}{2n_\rho}\frac{1}{\cos\theta}\right)^2 \tag{14}$$

Consequence: Because of the dependence of t_0 on n, the true medium slowness, Eq. (13) is no longer valid, so that the family of circles (14) looses its common tangent point; this means that I is imaged at *different* positions, one for each value of θ.

Moveout: Each image point moves *inward*, if $n_\rho > n$, or *outward*, if $n_\rho < n$, along the normal to the reflector leaving I. Figs.(6) and (7) display this behavior: the incorrect estimate of the slowness was modeled as follows

$$n_\rho = \rho\, n\ . \tag{15}$$

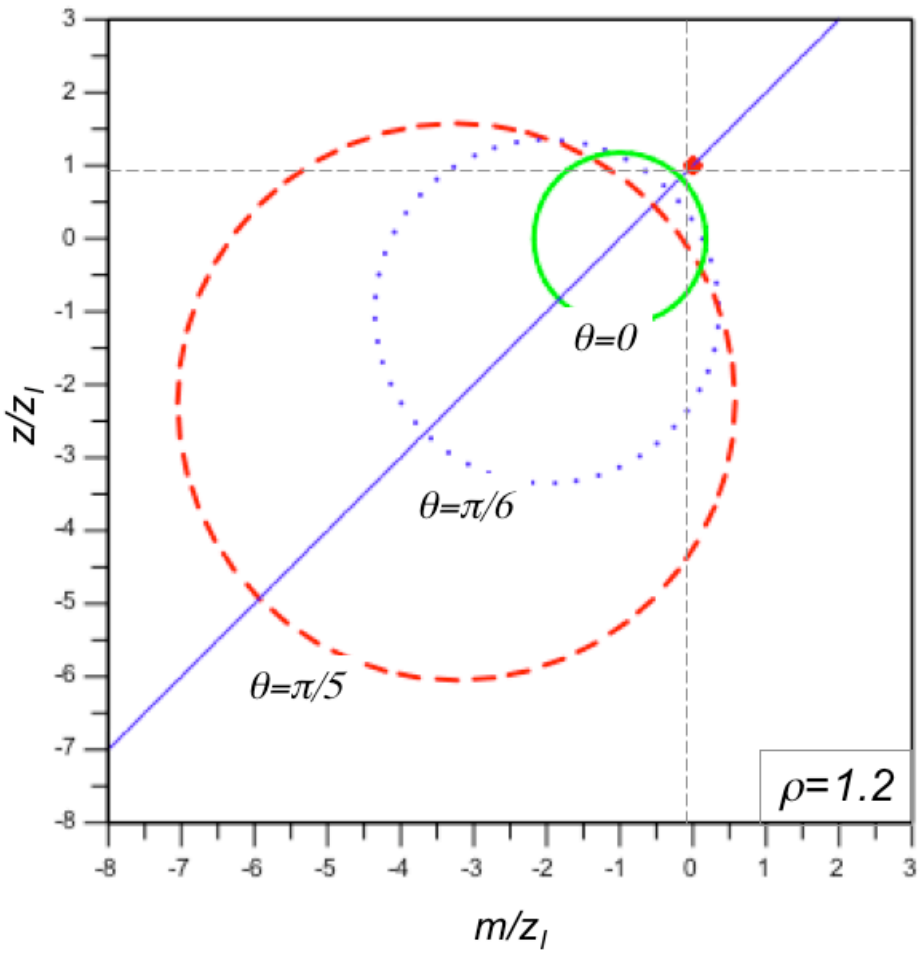

Figure 6: Wrong slowness value: each image point moves inward along the normal to the reflector

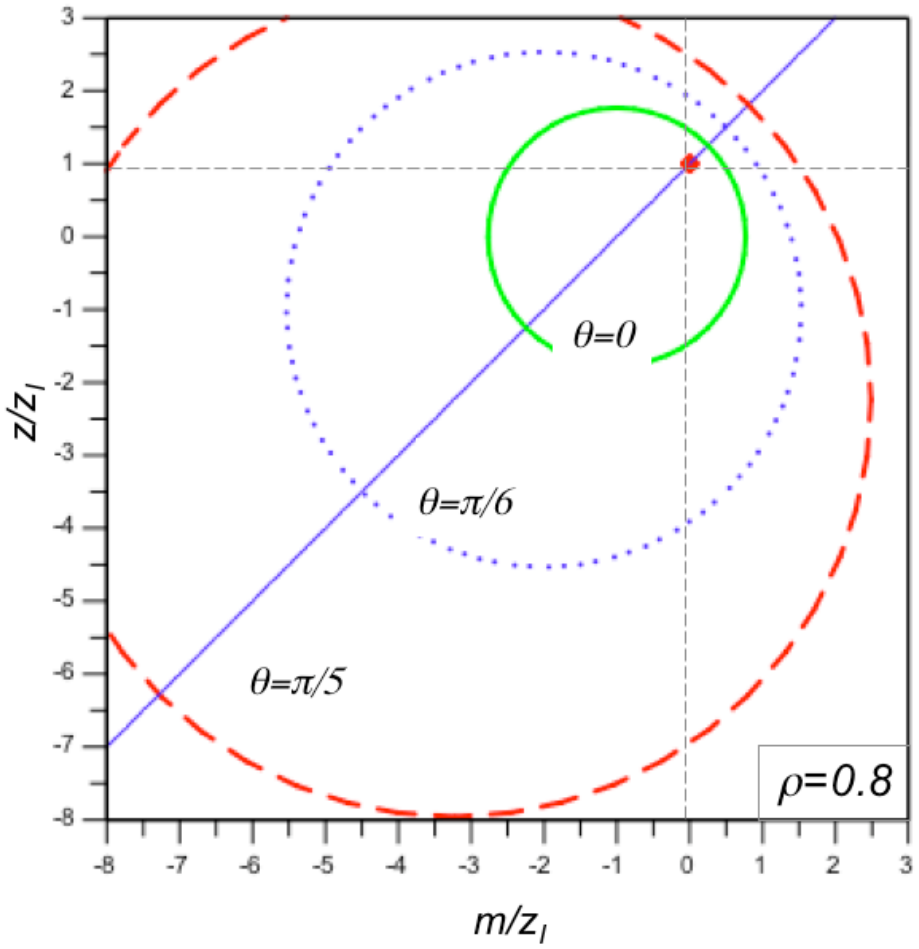

Figure 7: Wrong slowness value: each image point moves outward along the normal to the reflector

Vertical residual moveout analysis

Remark: From now on, we assume n_ρ is related to n through the scaling factor ρ.

Vertical moveout: Eq.(12) supplies the vertical component of the image of I, Fig.(3), migrated with the *improper* slowness (15):

$$z = -h_0 \tan\theta + \frac{t_0}{2\rho n}\frac{\cos\alpha_I}{\cos\theta} \ . \tag{16}$$

Substituting the expressions of h_0 and t_0, Eq.(7), into (16), we find the relation between the migration depth and the vertical coordinate of point I,

$$\frac{z}{z_I} = \frac{\cos^2\alpha_I - \rho\sin^2\theta}{\rho\left(\cos^2\alpha_I - \sin^2\theta\right)}, \tag{17}$$

controlled via the scaling factor ρ and the scattering angle θ (Biondi and Symes, 2004). Denoting by z_0 the depth at *normal* incidence, $\theta = 0$, from Eq.(17) we can write:

$$z_0 = \frac{z_I}{\rho}, \qquad \frac{\Delta z_{RMO}}{z_0} = \frac{(1-\rho)\sin^2\theta}{\cos^2\alpha_I - \sin^2\theta}. \tag{18}$$

$\Delta z_{RMO} = z - z_0$ is called the *residual* moveout along the vertical direction.

Improper slowness: A wrong migration slowness introduces a moveout with respect to the scattering angle θ, a situation illustrated by Fig.(8).

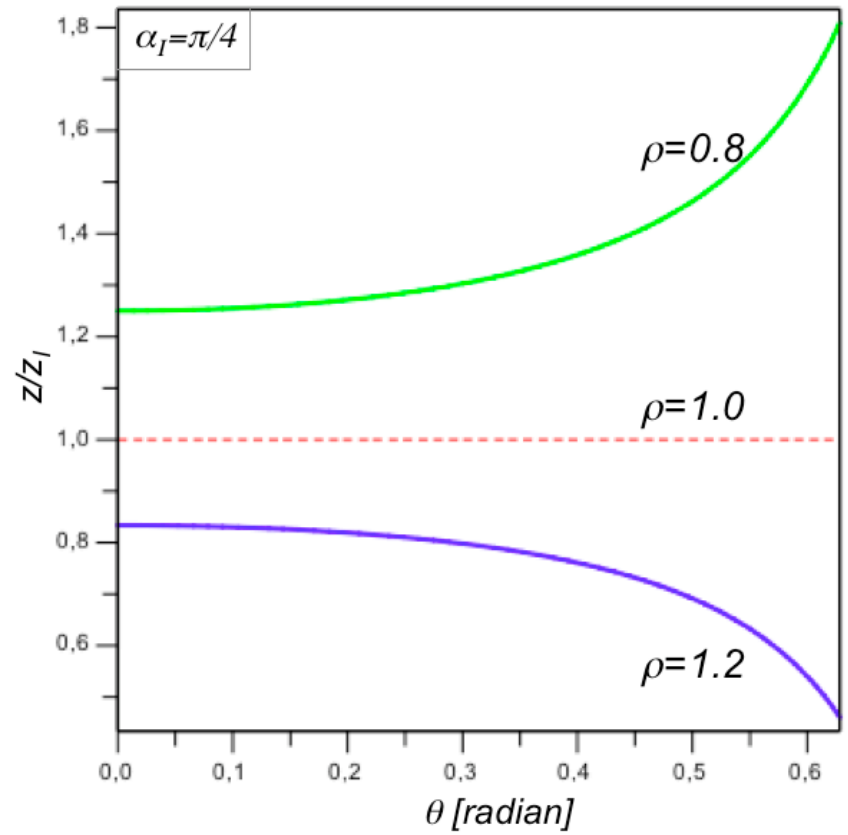

Figure 8: Migration with two improper slowness values: mispositioning of the vertical component of the image point.

An approximation: With narrow scattering angles, by re-writing Eq.(17) as a function of $\tan^2\theta$ and expanding the resulting expression in Taylor series, we find

$$\frac{z}{z_I} = \frac{1}{\rho}\left\{1 + \frac{\rho-1}{\cos^2\alpha_I}\left[\tan^2\theta + \tan^2\alpha_I \;\; \tan^4\theta + \tan^4\alpha_I \tan^6\theta + \cdots\right]\right\} \qquad (19)$$

with a truncation error decreasing *fast* when α_I tends to zero. The validity of (19) truncated to the forth order, here also expanded in θ, is illustrated in the two examples of Fig.(9):

$$\frac{z}{z_I} = \frac{1}{\rho}\left[1 + \frac{(\rho-1)}{\cos^2\alpha_I}\tan^2\theta\right] + O(\tan^4\theta)\ , \quad \frac{z}{z_I} = \frac{1}{\rho}\left[1 + \frac{(\rho-1)}{\cos^2\alpha_I}\theta^2\right] + O(\theta^4). \quad (20)$$

Remark: The agreement between (20) and the exact expression (17) is remarkably better for the approximation in θ; in both cases, the agreement increases as ρ tends to one.

Beyond to the second-order term in $\tan\theta$, Eq. (19) contains even powers of $\tan\alpha_I$; this means, for small dip angles, both approximations (20) provide a good estimate of the residual moveout even for reasonably large deviations of θ around zero.

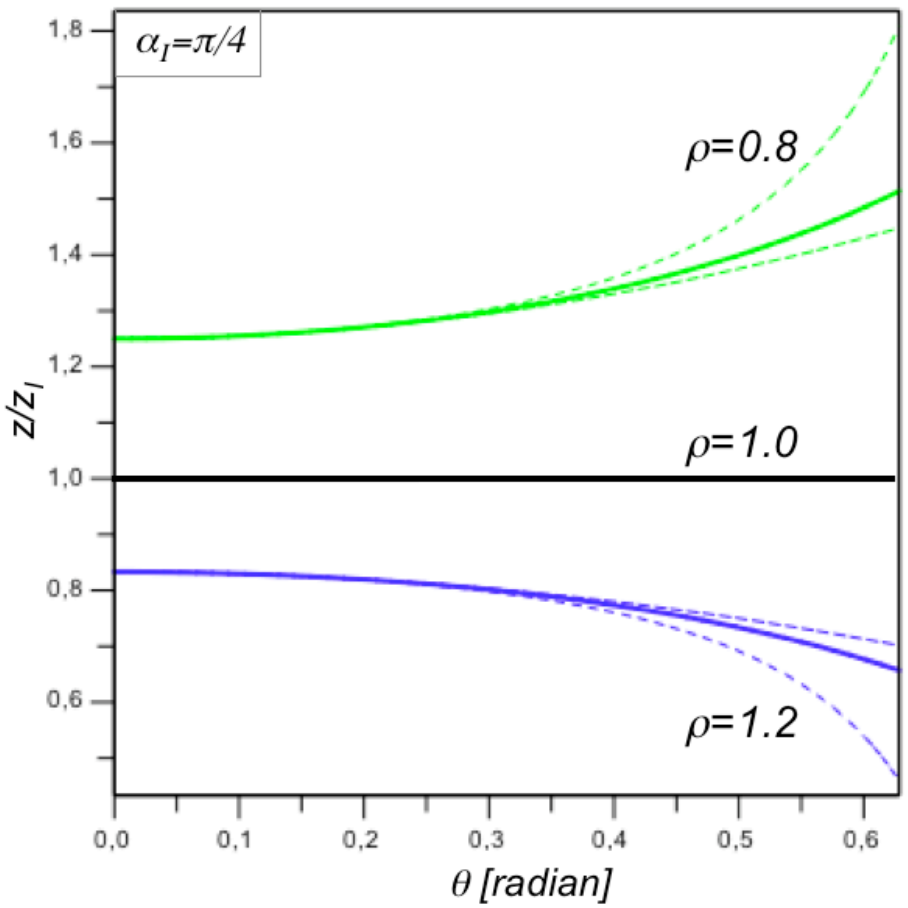

Figure 9: Comparison between the true moveout formula (solid lines) and two second order approximations, one in $\tan\theta$, the least accurate, and one in θ, the *best*.

Part III: False primary reflections and image mispositioning

Migration of a false primary reflection

So far, we have assumed t_0 is the time of flight of a *primary event* echoed at I, a point lying on a reflector with dip angle α_I, Fig.(2). The acquisition parameters, m_0 and h_0, and the length of the ray path, $t_0/2n$, are defined by the scattering angle θ of the primary event, Eqs.(7).

False primary event: The problem of a *multiple event* of order M, identified as a primary reflection, is here addressed. I provide the moveout expression referred to the scattering angle θ in the case of a dipping, *planar* reflector, Fig.(10).

Planar reflector: The time of flight of a multiple event for a planar reflector with a dip angle $|\alpha_I| < \pi/2$, satisfies

$$\left(\frac{t_M}{t_0}\right)^2 = \cos^2\theta \left\{\frac{\sin\left[(M+1)\alpha_I\right]}{\sin\alpha_I}\right\}^2 + \sin^2\theta \left\{\frac{\cos\left[(M+1)\alpha_I\right]}{\cos\alpha_I}\right\}^2, \qquad (21)$$

where the order, $M = 0, 1, 2, \cdots$, denotes the number of *bounces* with the acquisition surface (F. K. Levin, 1971). For the primary reflection $M = 0$.

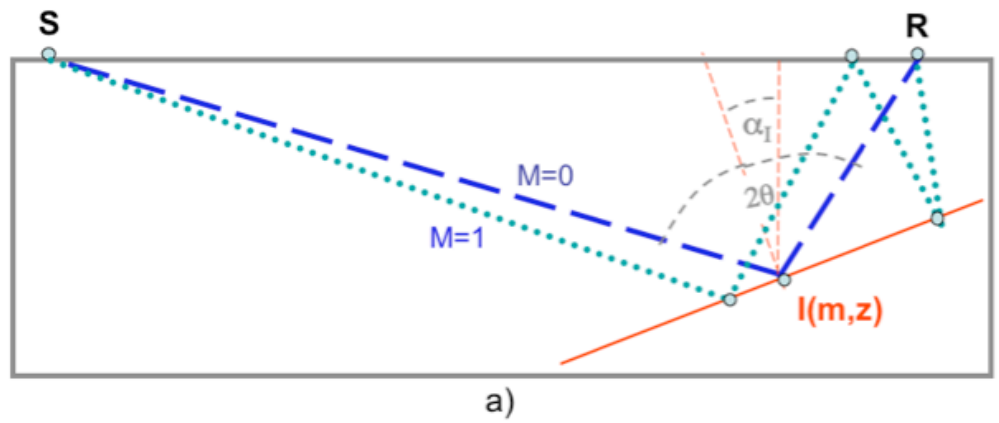

a)

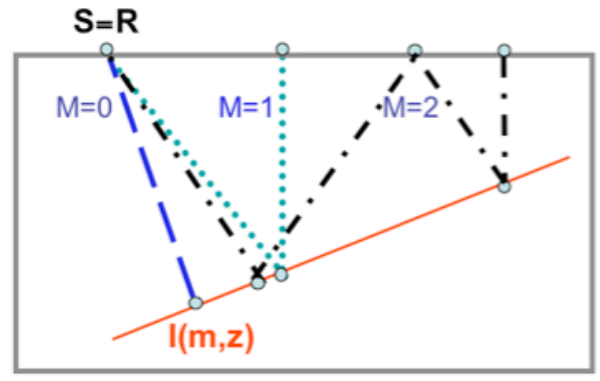

b)

Figure 10: Primary reflection (M=0), first (M=1) and second (M=2) order multiples bouncing between the surface and a dipping, planar interface: a) $\theta \neq 0$, b) $\theta = 0$.

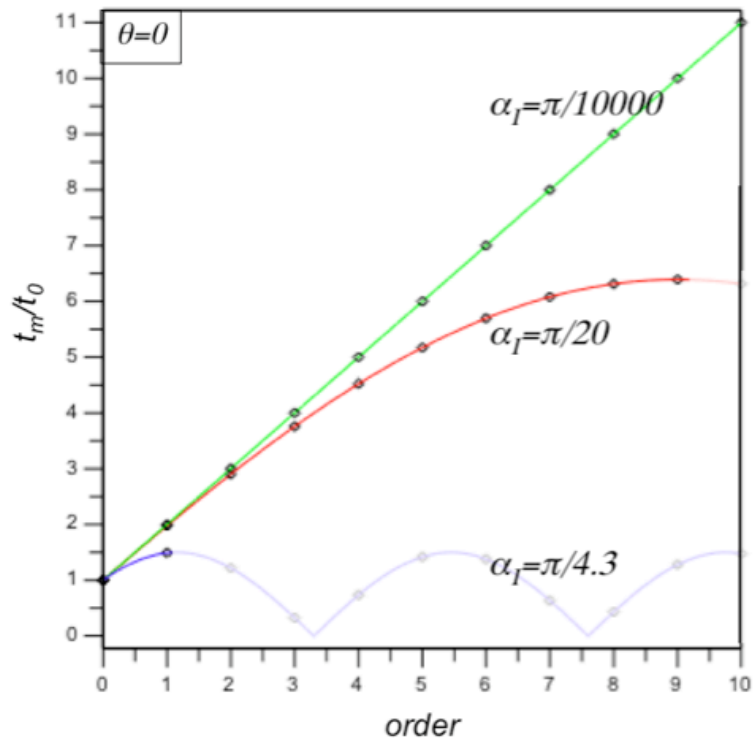

Figure 11: Relative time of flight of multiple events for a zero-offset acquisition and three dip angles.

Remark: Because $t_0 \leq t_M$, the only physically meaningful values of M are those for which (21) is monotonically increasing.

Image mispositioning after migration

Image moveout: After substitution of t_0 with t_m into Eq.(12), the modified coordinates of the migrated image are written

$$m = m_0 + \frac{t_M}{2n}\frac{\sin\alpha_I}{\cos\theta}\ , \quad z = -h_0\tan\theta + \frac{t_M}{2n}\frac{\cos\alpha_I}{\cos\theta}\ , \ |\theta| < \pi/2 - |\alpha_I|. \qquad (22)$$

Since $t_M \geq t_0$, we see that the *improper* response of I, once migrated, moves *outwardly* along the normal to the reflector.

Vertical moveout: Eqs.(22) provide the vertical displacement of the image of I caused by the improper implementation of (21). Using (7), the vertical moveout can be written as function of θ,

$$\begin{aligned}\frac{z}{z_0} &= \left\{-\tan^2\theta\frac{\sin\alpha_I}{\sin\left[(M+1)\,\alpha_I\right]}+\right.\\ &\left.\cos^2\alpha_I\sqrt{(1+\tan^2\theta)\left[1+\tan^2\theta\left(\frac{\tan\alpha_I}{\tan\left[(M+1)\,\alpha_I\right]}\right)^2\right]}\right\}\times\\ &\frac{1}{\cos^2\alpha_I-\tan^2\theta\sin^2\alpha_I}\ ,\end{aligned}\tag{23}$$

where z_0, the depth at *normal* incidence, $\theta = 0$, is related to z_I, the vertical coordinate of I, through

$$\frac{z_0}{z_I}=\frac{\sin\left[(M+1)\,\alpha_I\right]}{\sin\alpha_I}\ ,\ \ M<\left\lfloor\frac{\pi}{2|\alpha_I|}\right\rfloor\ ,\tag{24}$$

a function plotted in Fig.(11). These two last relations show that a *false* primary event causes a vertical moveout that increases with θ, *spreading* the migrated image well beyond z_I. See Fig.(12).

There is one situation for which this migration model is a good approximation of reality, in *marine exploration* over a slope.

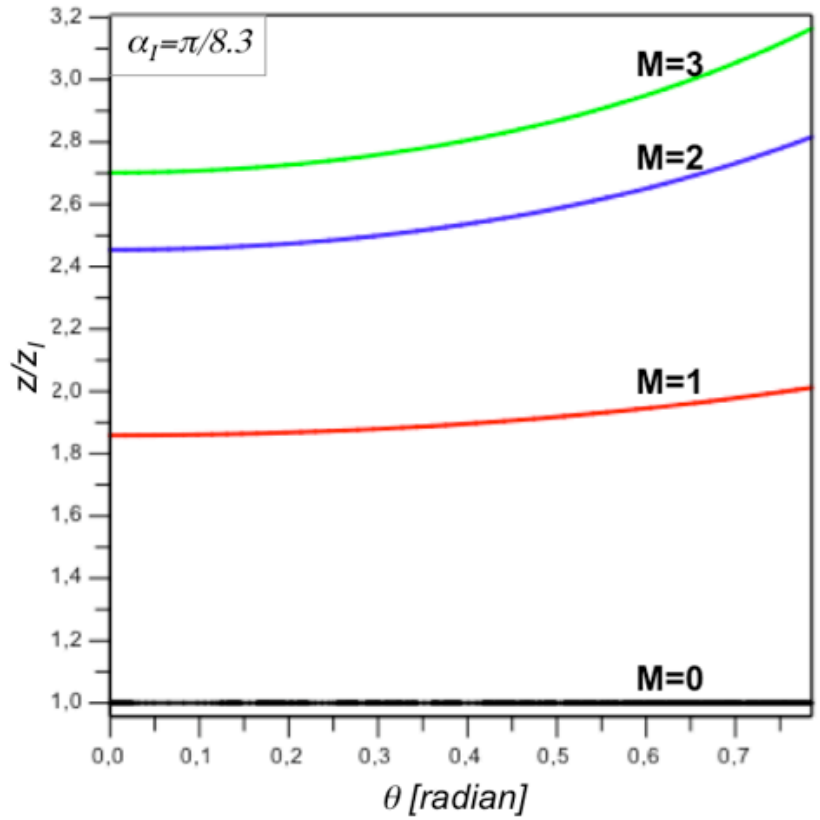

Figure 12: Dipping planar reflector: migration of false primary events and vertical mispositioning.

An approximation: Assuming a *narrow* scattering angle, the Taylor expansion of (24), truncated to the fourth order in $\tan\theta$, gives rise to

$$\frac{z}{z_I} = \frac{\sin\left[(M+1)\,\alpha_I\right]}{\sin\alpha_I}\left\{1+\frac{1}{2}\left(\frac{\sin\alpha_I-\sin\left[(M+1)\alpha_I\right]}{\cos\alpha_I\sin\left[(M+1)\alpha_I\right]}\right)^2\tan^2\theta+O(\tan^4\theta)\right\}\ . \quad (25)$$

Eq.(23) can also be expanded in θ:

$$\frac{z}{z_I} = \frac{\sin\left[(M+1)\,\alpha_I\right]}{\sin\alpha_I}\left\{1+\frac{1}{2}\left(\frac{\sin\alpha_I-\sin\left[(M+1)\alpha_I\right]}{\cos\alpha_I\sin\left[(M+1)\alpha_I\right]}\right)^2\theta^2+O(\theta^4)\right\}\ . \quad (26)$$

The agreement between these two approximations and (23) is illustrated in the example of Fig.(13), which also shows that, comparing the expansions to the second order, Eq.(26) is more accurate than (25).

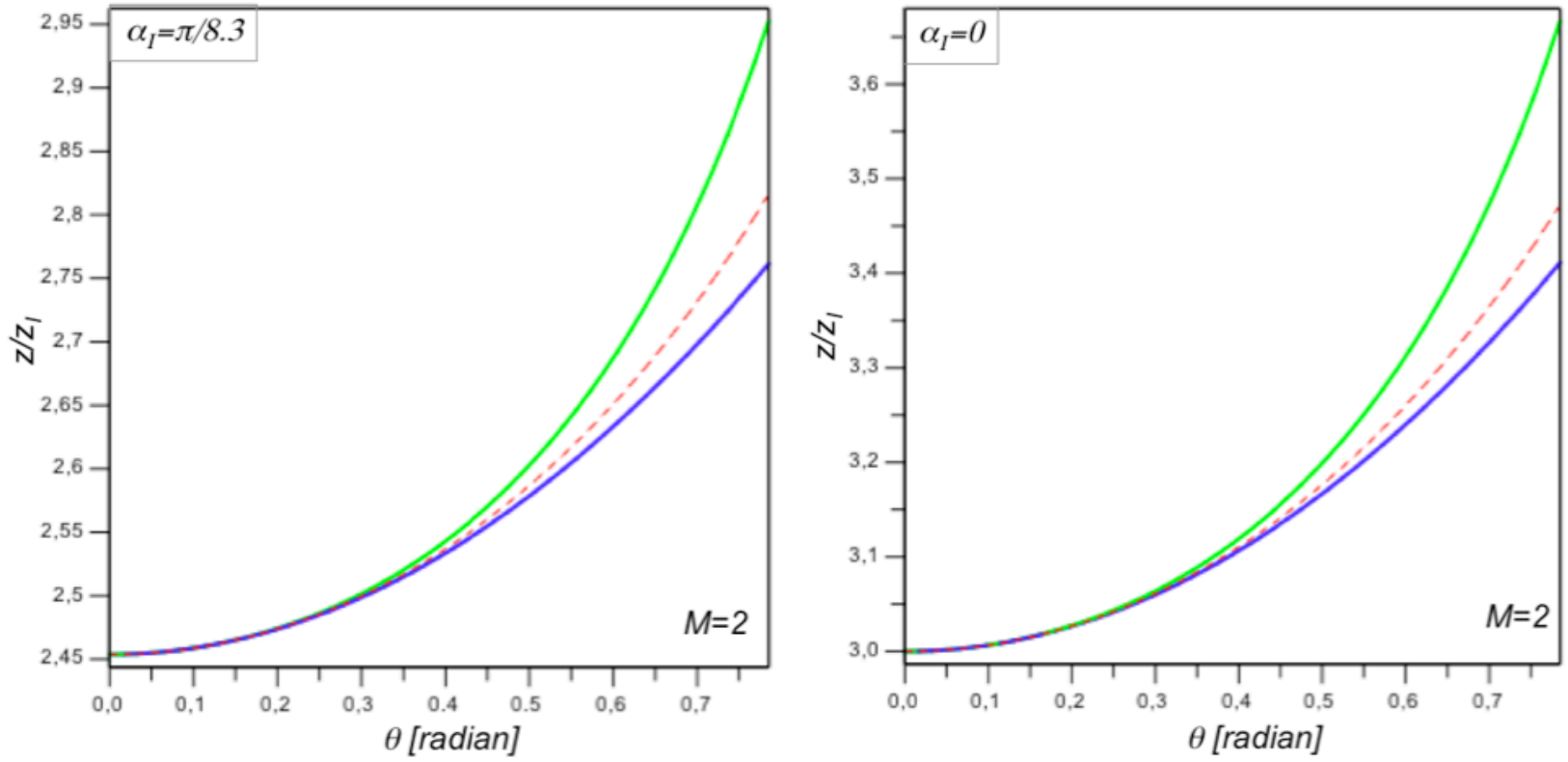

Figure 13: Comparison between the moveout formula (dashed line) and the two second order approximations, one in $\tan\theta$, the least accurate, and one in θ, the best.

The horizontal reflector: Leting α_I go to zero, Eq.(23) provides the vertical moveout for a point I lying on a horizontal plane, subject to a primary event with a scattering angle θ:

$$\lim_{\alpha_I \to 0} \frac{z}{z_I} = -\tan^2\theta + \sqrt{(1+\tan^2\theta)\left[(M+1)^2 + \tan^2\theta\right]}\ . \tag{27}$$

Small scattering angles: As expected, to the second order, the Taylor expansion of (27) takes the same form, both in $\tan\theta$ and θ:

$$\lim_{\alpha_I \to 0} \frac{z}{z_I(M+1)} = \begin{cases} 1 + \frac{1}{2}\left(\frac{M}{M+1}\right)^2 \tan^2\theta + O(\tan^4\theta), \\ \\ 1 + \frac{1}{2}\left(\frac{M}{M+1}\right)^2 \theta^2 + O(\theta^4). \end{cases} \tag{28}$$

The comparison between these two approximations and (27) shows that the expansion to the second order in θ is more accurate, Fig.(13).

Remark: The form of both Eqs.(28) has been conjectured (Sava and Guitton, 2005) using the analogy with the migration velocity analysis and the resulting Eq.(20).

General conclusion

In this work, I have discussed the problem of the image mispositioning in the depth-angle domain, a question which raises when the migration slowness is improperly known or when a multiple reflection is processed as a primary temporal event. In both cases, I only considered a homogeneous medium with a unique dipping reflector, a situation allowing the exact analysis of the error moveout, a function of the scattering angle.

The main *open question* is the extension of the derived results to the case of an non-homegeneous medium. In other words, is the general form of the approximated error moveout, namely $z/z_I = a + b\tan^2\theta$, preserved - at least for narrow scattering angles - in a complex stratigraphy?

Some empirical studies tend to give a positive answer that needs, however, more validation tests (Biondi and Symes, 2004, and Sava and Guitton, 2005), in particular for the 3D case.

References

- B. Biondi and W. Symes, 2004,*Angle-domain common-image gathers for migration velocity analysis by wavefield-continuation imaging*, Geophysics, **69**, 1283-1298.
- S. Fomel, 2003, *Angle-domain seismic imaging and the oriented wave equation*, SEG International Exposition and 73^{rd} Annual Meeting.
- F. K. Levin, 1971, *Apparent velocity for dipping interface reflections*, Geophysics, **36**, 510-516.
- P. Sava and A. Guitton, 2005, *Multiple attenuation in the image space*, Geophysics, **70**, V10-V20.
- R. H. Stolt and A. B. Weglein, 1985, *Migration and inversion of seismic data*, Geophysics, **50**, 2458-2472.